Corona discharges: fundamentals and diagnostics

E.M. van Veldhuizen, W.R. Rutgers
Faculty of Applied Physics, Technische Universiteit Eindhoven
PO Box 513, 5600 MB Eindhoven, The Netherlands

Introduction

Corona discharges are discussed in this paper as one example of pulsed atmospheric discharges. Other configurations used are the dielectric barrier and the packed bed reactor. Here only the volume discharge will be discussed and not the surface discharge that also plays a role in these last two cases.
The paper is divided in two parts. Fundamental processes that are important in corona discharges are treated in the first section. The characteristic properties of the corona will show up clearly here, its fast development in time and space being a dominating feature. It will also be indicated where knowledge of the processes involved is still marginal or even missing.
The second part gives an overview of experimental diagnostics that are in use to obtain data of the propagating discharge. Commonly used methods are treated as well as state-of-the-art developments.

General aspects of discharges at atmospheric pressure

Discharges at a pressure of 1 bar have several appearances. Lightning is one of them and although it is known with most people it is difficult to describe the lightning discharge in detail. In terms of discharges it is an arc with rather short duration and high power density. Arcs are also used in a more controlled way for instance for welding, high voltage circuit breakers or certain types of lamps. Arcs with duration in the microsecond range are usually called sparks and they are often observed at switching contacts. In case of high voltage applications breakdown can cause severe damage. Even shorter discharges can be created which in fact stop before they are completed in to arcs. These are sometimes called transient discharges and have typical time duration in the range of nanoseconds. There are two ways to create these discharges. A dielectric layer can cover one or two of the electrodes in the discharge gap. At a sufficiently high voltage between the electrodes the discharge starts in the gas volume. It spreads out until it reaches the electrodes but at the dielectric it builds up a space charge that cancel the applied electric field. At that moment the discharge stops. This discharge is usually called dielectric barrier discharge. The second method is to use an asymmetric electrode pair. Then the discharge develops in the high field region near the sharp electrode and it spreads out towards the cathode. In this case there are two possibilities to avoid the transition in to an arc. First the voltage can be made low enough to stop the spreading of the discharge somewhere before the cathode is reached. Second one can stop or lower the voltage when the cathode is reached. In the second way more energy can be put on to the discharge but it is more difficult to make the power supply. This type of discharge is called corona. It is a positive corona when the electrode with the strongest curvature is connected to the positive output of the power supply and a negative corona when this electrode is connected to the negative terminal of the power supply. In corona discharges at relatively low voltages the discharge stops itself due to the build up of space charge near the sharp electrode. This space charge then disappears due to diffusion and recombination and a new discharge pulse appears. This is the self-repetitive corona and it occurs in the positive and in the negative case.

Atmospheric discharges are under investigation since two decades for many environmental purposes [1]. The corona discharge and the barrier discharge are both good candidates in these applications. It is still an open question which type of discharge has the highest efficiency in plasmachemical applications. It appears that the barrier discharge can achieve higher electrical power densities but the corona discharge may be easier scalable to large gas flows. The barrier discharge is more complicated since it is a combination of a gas discharge and a surface discharge along the dielectric. This article is restricted from now on to the corona discharge. Only the positive corona will be discussed in detail since it was shown in many cases to be more effective than the negative case.

Development steps

The growing of the (positive) corona discharge will now be treated in more detail. Several steps are part of this process:

1. An asymmetric electrode configuration must be made
2. A high voltage must be applied
3. Some free electric charge must be present
4. An avalanche must build up and leave behind a space charge area
5. Photons from the avalanche create new charge carriers outside the space charge area
6. New avalanches develop closer to the cathode

Ad. 1: Field enhancement near one electrode is required. The most common methods used in practice for this purpose are point-to-plane and wire-in-cylinder geometries. The point-to-plane is convenient for comparisons with model calculations and the wire-in-cylinder is most suitable for gas treatment where the residence time in the cylinder is an important parameter especially for the plasmachemical processes. Surface roughness can be expected to be important for field enhancement. Recent photographs taken at TUE show that the streamer is connected to the anode on a spot with a dimension in the order of one pixel of the CCD camera used, i.e. ~20 μm. The corona current is ~1 A, so this leads to a current density of ~3 10^9 A/m^2. Erosion (or sputtering) of the anode can be expected in such a case. In laboratory experiments this is not a problem and these aspects have not been studied in detail. For large-scale, long-term application it may become an important factor in maintenance cost.

Ad. 2: The breakdown field strength in a uniform gap with atmospheric air is in the order of 3 kV/mm. This implies that a free electron gains on average several eV of energy from the field in-between collisions. The ionization energy of air molecules is roughly 10 eV. Nevertheless there will be electrons in the tail of the electron energy distribution function that have enough energy to cause ionization. Near a surface roughness much higher field strengths are readily obtained. Field emission cannot occur, however, because the electrons are drawn towards the anode.

Ad. 3: The first electron, which should start the discharge, can be provided in two ways. Cosmic radiation produces them at a rate of ~1 el/mm^{3}s. This leads to rather low background electron densities of 10^3-10^6 el/cm^3. This can imply that it takes some time for an electron to be at the right place, i.e. a region where the electric field is high enough. This time is called inception time lag and in practice it varies from about 1 ns to many microseconds. Another process that can provide electrons is field detachment from negative ions. This effect can be important when ions of a previous discharge are still present. It occurs in the self-repetitive DC corona and it causes the streamer to choose the path of its predecessor. In most applications of pulsed corona it does not occur due to the low repetition rate (~100 Hz).

Ad. 4: When the first electron has caused an ionization there are two electrons left that again start moving in the electric field and ionize again etc. In this way the so-called avalanche builds up. This process continues until the space charge of the slow ions that are left behind cancels the applied electric field. The avalanche can also stop at the anode before it is complete. In such a case the avalanche extinguishes. The length required to build up a complete avalanche is called the critical length; at 1 bar it is in the order of 1 mm [2].

Ad. 5: The space charge region cancels the field between itself and the anode, but it enhances the field in the direction towards the cathode. A free electron at the right position in this area can start a new avalanche. However, the background electron has by now disappeared from the gap due to drift. A process that can provide new electrons is photoionization. This is caused by VUV resonance photons of N_2 that are absorbed by O_2. Only the photons that originate in the tail of the lineprofile of N_2 can travel far enough, but in principle one electron is sufficient. This explanation cannot be used for discharges in e.g. pure N_2 or noble gases. Unfortunately however, data on photoionization in theses cases is unavailable. In case of N_2-O_2 mixtures only one paper is known which gives quantitative data [3]. Computer models of streamer propagation are also made without photoionization. An artificial background electron density is then required for starting new avalanches. Although such a background is not realistic, the results are very similar to models that do include photoionization.

Ad. 6: The electrons of the new avalanche cancel the previous space charge but they create a new one closer to the cathode. It is found that a so-called stability field of 5 kV/cm is sufficient to continue the propagation of the streamer channel. A cathode sheath builds up when the avalanche reaches the cathode [4]. This process is usually not considered in streamer propagation models. If the power supply can continue to deliver current the temperature of the channel will increase due to Joule heating, then its resistance will drop and the discharge may develop in to an arc.

In this paper the situation is considered that the corona current stops after the streamer head reaches the cathode. Many processes continue to occur in the gap after the discharge has stopped. The ones that are often important for further physical and chemical processes are:

1. Attachment
2. Recombination
3. Diffusion
4. Vibrational relaxation
5. Metastable quenching
6. Radical reactions

Ad. 1: Attachment is the formation of negative ions when low energy electrons combine with atoms or molecules. Not all particles form negative ions, examples are the noble gases and also nitrogen molecules. Some molecules that easily form negative ions are O_2, H_2O and CO_2. The conductivity of a plasma is strongly influenced by the capturing of low energy electrons: the light and mobile electrons are replaced by heavy ions. Therefore the field strength for sustaining a certain current is much higher in an electronegative gas. This effect partly explains e.g. why a small amount of water can have a big impact on a noble gas discharge or the difference between dry air and flue gas.

Ad. 2: Recombination of positive ions and electrons (or negative ions) leads back to the neutral gas as before the discharge pulse. It can cause some additional effects such as the

emission of recombination radiation which can be used to determine the electron energy if its intensity is sufficient. In case of a corona discharge this is not to be expected. Further it can lead to the formation of excited states that have high chemical activity. The recombination time in the atmospheric corona discharge is estimated to be in the order of 1 μs. It has not been measured up to now. The time interval required for a corona pulse in order not to notice its predecessor is found in experiments to be in the order of 1 ms. This is probably due to negative ions and/or metastables that have much longer lifetimes than electrons.

Ad. 3: The active particles in a corona discharge are formed in a thin channel (diameter ~200 μm). It is often the intention to treat the whole gas volume, so one may wonder if diffusion is able to spread the radicals significantly. From Schlieren pictures (see next section) it is seen that the streamer diameter increases to ~2 mm in 200 μs. So, this increases the treated volume but still a single discharge pulse treats only a volume fraction in the order of 10^{-3}. This explains why in practice a residence time of several seconds is usually required for a complete treatment. The turbulence created by the corona pulses probably helps to mix the gas but this effect has not been studied in detail up to now.

Ad. 4: The high-energy electrons in the streamer head cause ionization and excitation to higher electronic states. The most important example is the $N_2(C)$-state because it leads to the UV emission of the so-called Second Positive System. The excitation also leads to high vibrational relaxation by which these states decay through collisions to rotational and translational excitation. This is the same as saying that the gas is heated. Emission spectroscopy can give quantitative results about these processes (see next section).

Ad. 5: Excited metastable states cannot lose their energy by emission of a photon. Another process to take away energy from them is by collisional quenching. Metastables are often close to resonant levels, so a collision with a low energy electron can cause them to become resonant, lose the energy within ~1 μs by emitting a VUV photon and become a ground state. It is also possible that they transfer all their energy to a different molecule. In this way quenching of a N_2 metastable can cause dissociation of a water molecule. This process is considered to give an important contribution to the formation of OH radicals in humid air or flue gas. No quantitative studies are available at present, however.

Ad. 6: Radicals are formed by electron impact dissociation of molecules in the streamer head region. The dissociation energy is usually somewhat lower than the ionization energy. Primary radicals are the ones created directly by these collisions, e.g. O, H, OH and N. They may react rapidly with molecules to form secondary radicals such as HO_2 or O_3. If contaminations such as SO_2 or NO are present O, HO2 and O3 can oxidize them to acids. The N radical can reduce NO to N_2. How much this happens depends on the gas composition. This is one of the major application areas of corona discharges [1].

Diagnostics

1. Cloud chamber tracks

The first recordings of avalanches have been made by Raether [5]. He used a cloud chamber to grow droplets around the ions that are left behind. These droplets are photographed through light scattering. Such pictures are extremely sensitive but have, however, no time resolution. Fig. 1 is obtained from the original paper by Raether from 1939. He used a plan parallel gap with N_2 at 150 Torr. The length of the avalanche is of the order of 1 cm.

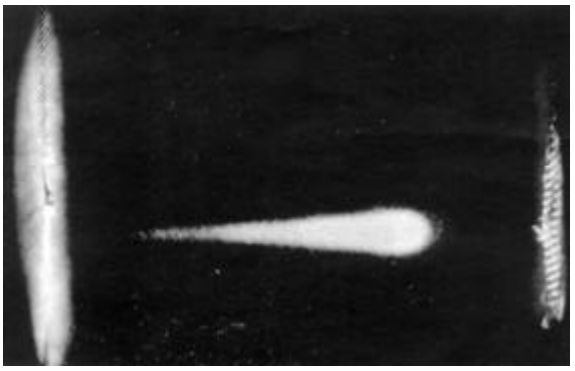

Fig. 1: Cloud track picture of a single avalanche, cathode at the left (by H. Raether, [5]).

2. Streak pictures

The next method, used by Wagner, is streak photography using an image-intensified camera [6]. The pictures obtained with such a system show one spatial dimension versus time. Figure 2 gives an example.

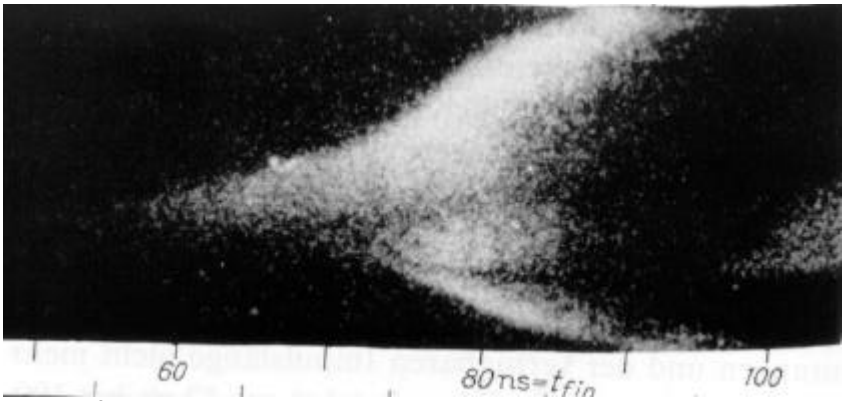

Fig. 2: Streak picture of cathode (bottom) and anode (top) directed streamer in a 30 mm plane gap with 378 Torr N_2 (by K.H. Wagner, [6]).

In fig. 2 it can be seen that in the case of plane electrodes the streamer starts in the middle of the gap and it develops towards cathode and anode. Two phases of developments are distinguished: from 60 to 70 ns with a propagation velocity of ~2-3 10^5 m/s and from 70 to 80 the speed becomes ~10^6 m/s.

3. Photography

The streamer discharge is difficult to access by experiments due to its transient nature. Its total duration is in the order of 10 ns and the streamer head moves along its own thickness in 0.1 ns. This resolution is still not obtained with state-of-the-art cameras. Present day intensified CCD camera's can be gated down to about 1 ns. The sensitivity of these cameras is becoming close to that of photomultipliers, this is quite sufficient to allow single shot exposures. An example is given in fig. 3, which is a photograph of a point-plane corona discharge in a 25 mm gap in ambient air using a voltage pulse of 25 kV with a rise time of 30 ns. The camera used here is an Andor Technology ICCD-452 having the following specifications:

- 1024 x 1024 pixels
- pixel size 13 µm x 13µm

- sensitivity 180-850 nm
- minimum optical gate 0.8 ns
- full width at half maximum 21 μm
- gain up to 3600

Fig. 3: Pictures of streamer propagation in a point-to-plate gap using a 0.8 ns intensifier gate, real size per frame ~3x3 cm^2 (picture by A.H.F.M. Baede)

Figure 3 shows three pictures at different trigger moments. The time lap between the left and the right pictures is ~40 ns. This value cannot be determined very accurate in the present set-up used because of jitter in the power supply and the corona initiation. The dark spots of the streamer heads are overexposed in these pictures; therefore they look larger than they are. An analysis of their full width at half maximum shows a value of 150 μm for all streamers observed under this condition [7]. Figure 4 shows similar pictures in a wire-cylinder gap with a cylinder having an inner diameter of 290 mm. A voltage pulse of 100 kV is used here having a rise time of 20 ns.

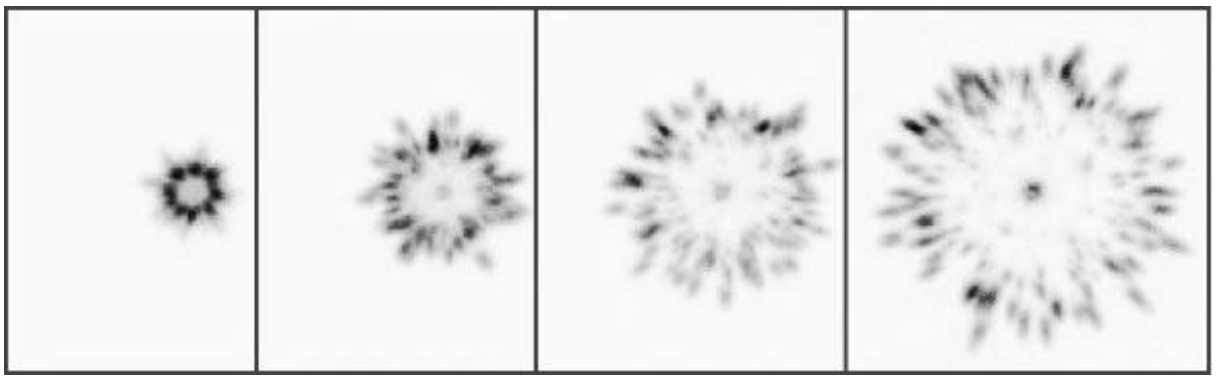

Fig. 4: Four stages in the expansion of a corona discharge in a 29 cm cylinder. Opening time 5 ns at 10, 20, 30 and 40 ns after the initial rise of the voltage pulse of 200 kV with 20 ns rise time, real size last frame ~30x30 cm^2 (by P.P.M. Blom, [8])

Figures 3 and 4 show similarities in the way the streamer heads move from anode to cathode but in the streamer diameters are quite different, in fig. 3 they are ~0.2 mm and in fig. 4 ~1 cm. Comparing these figures to 2-D modeling of streamer propagation one finds that the results of fig. 3 are close to those obtained by simulations. The situation of fig. 4 is different due to the extreme rate of rise of the voltage. It resembles the fast ionization wave (FIW) where electron energies are higher than in the corona discharge [9]. This FIW is the transition region to runaway electrons that can have keV's of energy as has been measured by detection of X-rays [10].

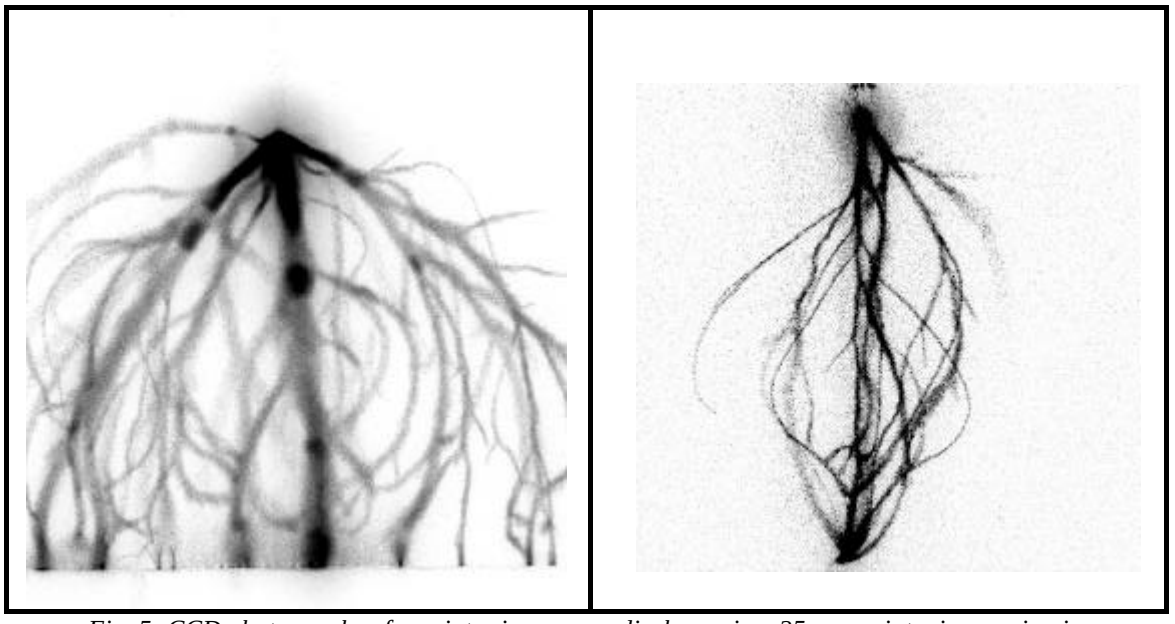

Fig. 5: CCD photographs of a point-wire corona discharge in a 25 mm point-wire gap in air. Left: view perpendicular to wire, right: view parallel with wire

.

Figure 5 shows two examples of pictures taken with exposure times of 100 ns, i.e. a time integrated picture of the discharge crossing the gap. In the left part one sees that the streamers spread out to a width that is larger than the point-wire distance. The right figure shows how the streamers bend out in the middle of the gap but they redirect towards the wire.

4. Schlieren photography

The path created by the corona streamer has a composition that is different from the surrounding gas. It can also have an enhanced temperature. Therefore its refractive index differs from its background. Such a difference can be visualized by Schlieren photography. This can be performed in three ways: 1. standard Schlieren methods are sensitive to the gradient in the refractive index, dn/dx, 2. interferometry, which is related directly to the refractive index n and 3. shadowgraphy which is proportional to d^2n/dx^2 [2, 11]. Figure 6 is obtained by a standard knife-edge method.

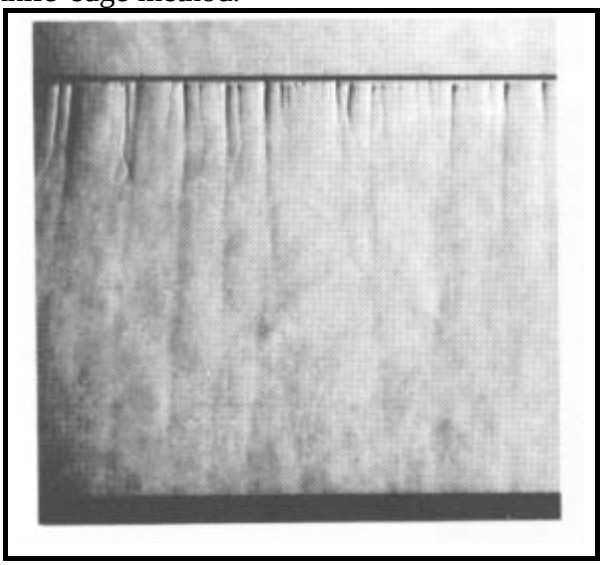

Fig. 6: Schlieren photograph of wire-plane pulsed corona taken 100 ns after the voltage pulse (by Y.L.M. Creyghton, [2])

The remarkable result of Schlieren pictures of a corona discharge is that its appearance is most clearly 50 to 100 μs after the voltage pulse. Within 1 μs the streamer paths are not observed. The explanation for this is that the fast electrons first cause ionization and vibrational excitation that does not affect n. After vibrational de-excitation to rotations and translations the streamer channel gets heated and shows up more clearly. A time constant of 100 μs for this process is reasonable.

5. Emission spectroscopy

The optical emission of the corona streamer can be analyzed by spectroscopic techniques. Monochromators have sufficient resolution for a discharge at 1 bar but main problems are the low intensity and the short duration. A technique that is well suited in this case is the time-correlated single-photon counting method. It uses an optical trigger to determine the timing of the photon to be counted. A time-to-amplitude converter can be included to obtain a time resolution down to 0.1 ns. Several slightly different version of this method are in use, not only for the pulsed corona [2, 12] but also for the self-repetitive discharge [13-15].

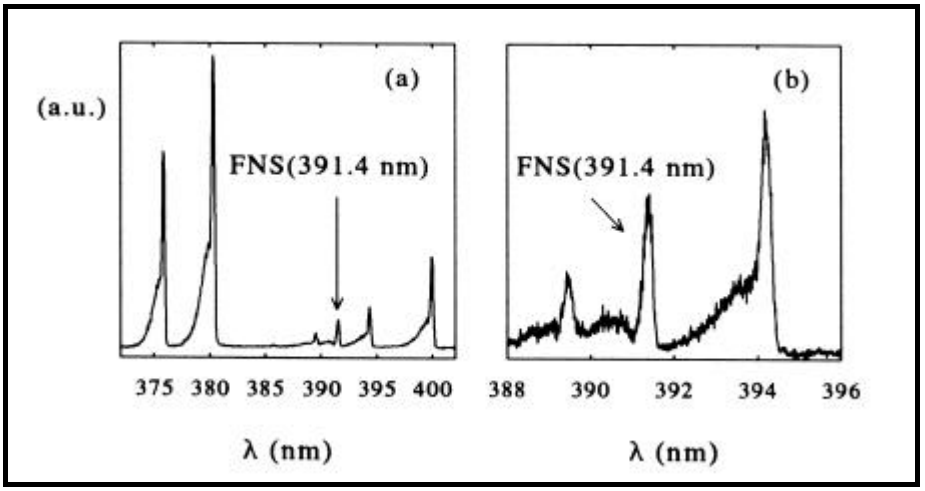

Fig. 7: Emission spectrum of a pulsed corona discharge showing parts of N_2 SPS and FNS (by Y.L.M. Creyghton, [2]).

Figure 7 gives an example of a part of the nitrogen spectrum in the near UV. It shows part of the Second Positive System of N_2 and the First Negative System of N_2^+. Because these systems have very different excitation levels the ratio of their intensities is a measure of the electron energy. Using this effect one obtains ~10 eV for electrons in the streamer head [2].

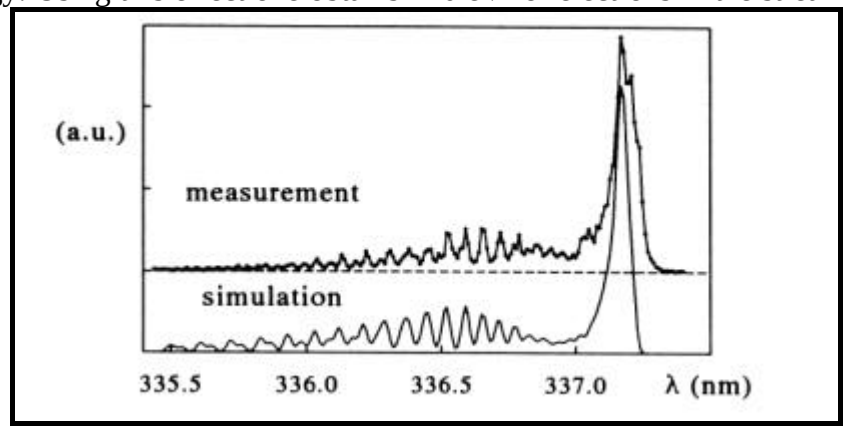

Fig. 8: Measured and calculated rotational structure of the N2 SPS (0-0) transition in the secondary streamer phase of a pulsed corona (by Y.L.M. Creyghton, [2])

In figure 8 the rotational structure of the SPS (0-0) transition is resolved. It is compared with a calculated spectrum with a rotational temperature of 350 K. The spectrum shown here is recorded in a time interval of 50-200 ns after rise of the voltage pulse, so the secondary streamer is observed [2]. It shows that the gas is still hardly heated at this instant.
The width of the measured spectral line can also be used. A nice example of it is given in [16] where the Stark broadening of the H-β line is used to determine the electron density. The result of 10^{15} cm^{-3} is, however, one order of magnitude higher than values obtained from simulations [1].

6. Absorption spectroscopy
Atoms and molecules can absorb light of specific wavelengths. The advantage of absorption is that it easily gives quantitative information on the lower level of the transition involved. Calibration is usually straightforward from known cross sections or gas mixtures. This method can be used to detect all kinds of species in a discharge (or any other gaseous system). Ozone is a well-known example but also NO, NO_2, SO_2 and NH_3 are easily determined [1, 17]. Short living excited states and radicals, created by the discharge can also be measured. A nice example is the OH ground state density in a tandem barrier discharge [18]. Absorption spectra can also be used to determine rotational temperatures [19].

7. Laser induced fluorescence
Although absorption spectroscopy is relatively easy it cannot be used in many cases because the absorption of low-density species is weak. The molecule that has absorbed radiation can emit this in other directions and also at other wavelengths, the so-called fluorescence. In that case using a strong source, e.g. a laser, can increase the signal. The sensitivity of this method is many orders of magnitude higher than the classical absorption technique. The first example of its use in a barrier discharge is the detection of OH radicals [20, 21]. Other examples are N_2^+ [22], $N_2(A)$ [23], NO [24], N [25].

Final remarks
The corona discharge at atmospheric pressure is in use and under investigation already for a long time. Its use with a pulsed power supply is of more recent date. From all information given above one may get the idea that the situation is well known. This is, however, not the case. Many processes are only estimated or assumed, e.g. field emission, photoionization, diffusion, recombination, and collisional de-excitation. The fact arising from this situation is that for e.g. values found for the electron density range from 3 10^{13} to 2 10^{15} cm^{-3}. For OH radicals very few measurements are available. In [18] a volume-averaged value of 10^{15} cm^{-3} is obtained. This implies a density inside the streamer that is much higher than values obtained from simulations [1].
So the problem that is faced is to make the results more quantitative. This must be done from theory and experiment since not all details can be measured using present day equipment. All methods mentioned above can be used for this purpose with detection possibilities that have only recently become available, e.g. generation-IV CCD-camera's. New techniques can probably be added. On can think of Coherent Anti-Stokes Raman Scattering to be used in rough environments. It is already being tested in barrier discharges [26]. Another possibility is Cavity Ringdown Spectroscopy, which is an extremely sensitive absorption technique that could be used to determine short living intermediate species.
The final aim should be to develop sufficient understanding of the discharge in order to predict and develop applications.

References

[1] E.M. van Veldhuizen (editor), *Electrical Discharges for Environmental Purposes: Fundamentals and Applications*, Nova Science Publishers, New York, 1999, ISBN 1-56072-743-8, 420 pages.

[2] Y.L.M. Creyghton, *Pulsed Positive Corona Discharges: Fundamental Study and Application to Flue Gas Treatment*, Ph.D. thesis TUE, Eindhoven, September 1994.

[3] G.W. Penney, G.T. Hummert, *Photoionization measurements in air, oxygen and nitrogen*, J. Appl. Phys. **41**(1970)572-577.

[4] I. Odrobina, M. Cernak, *Numerical simulation of streamer–cathode interaction*, J. Appl. Phys. **78**(1995)3635.

[5] H. Raether, *The development of electron avalanche in a spark channel (from observations in a cloud chamber)*, Zeitschrift fur Physik **112**(1939)464. (Reproduced in: *Electric Breakdown in gases*, J.A. Rees, The Macmillan Press, London, 1973).

[6] K.H. Wagner, *Vorstadium des Funken, untersucht mit dem Bildverstaerker*, Zeitschrift fur Physik **204**(1967)177.

[7] E.M. van Veldhuizen, A.H.F.M. Baede, D. Hayashi, W.R. Rutgers, *Fast imaging of streamer propagation*, APP Spring Meeting, Bad Honnef, 2001, p. 231-234.

[8] P.P.M. Blom, *High-Power Pulsed Corona*, Ph.D. thesis, Eindhoven University of Technology, ISBN 90-386-0250-2, 1997.

[9] S.M. Starikovskaia, A.Yu. Starikovskii, D.V. Zatsepin, *The development of a spatially uniform fast ionization wave in a large discharge volume***,** J. Phys. D: Appl. Phys. **31**(1998)1118-1125 .

[10] G.A. Mesyats, Yu.I. Bychkov, V.V. Kremnev, *Pulsed nanosecond electric discharges in gases*, Sov. Phys. Uspekhi **15**(1972)282-297.

[11] Y.L.M. Creyghton, E.M. van Veldhuizen, W.R. Rutgers, *Electrical and optical study of pulsed positive corona*, in: *Non-Thermal Plasmas for Pollution Control*, ed. by B.M. Penetrante and S.E. Schultheis, NATO ASI Series, subseries G, vol. 34, Springer, 1993, part A, p. 205.

[12] O. Motret, C. Hibert, S. Pellerin, J.M. Pouvesle, *Rotational temperature measurements in atmospheric pulsed dielectric barrier discharge – gas temperature and molecular fraction effects*, J. Phys. D: Appl. Phys. **33**(2000)1493-1498.

[13] K. Kondo, N. Ikuta, *Highly resolved observation of the primary wave emission in atmospheric positive-streamer corona*, J. Phys. D: Appl. Phys. **13**(1980)L33.

[14] F. Tochikubo, T.H. Teich, *Optical emission from a pulsed corona discharge and its associated reactions*, Jpn. J. Appl. Phys. **39**(2000)1343-1350.

[15] R. Brandenburg, K.V. Kozlov, P. Michel, H.-E. Wagner, *Diagnostics of the single filament barrier discharge in air by cross-correlation spectroscopy*, HAKONE VII, Greifswald, Germany, sept. 2000, p.189-193.

[16] E. Gerova, S. Muller, *Measurements of electron density in dielectric barrier discharges*, XXIII ICPIG, Toulouse, France, 1997, p. IV-120.

[17] I.P. Vinogradov, K. Wiesemann, *Classical absorption and emission spectroscopy of barrier discharges in N_2/NO and O_2/NO_x mixtures*, Plasma Sources Sci. Technol. **6**(19997)307.

[18] C. Hibert, I. Gaurand, O. Motret, J.M. Pouvesle, *[OH(X)] measurements by resonant absorption spectroscopy in a pulsed dielectric barrier discharge*, J. Appl. Phys. **85**(1999)7070-7075.

[19] M. Spaan, J. Leistikow, V. Schultz-von der Gatten, H.F. Döbele, *Dielectric barrier discharges with steep voltage rise: laser absorption spectroscopy of NO concentrations and temperatures*, Plasma Sources Sci. Technol. **9**(2000)146-151.

[20] J.J. Coogan, A.D. Sappey, *Distribution of OH within silent discharge plasma reactors*, IEEE Trans. Plasma Sci. **24**(1996)91-92.

[21] R. Sankaranarayanan, B. Pashaie, S.K. Dhali, *Laser-induced fluorescence of OH radicals in a dielectric barrier discharge*, Appl. Phys. Lett. **77**(2000)2970-2972.

[22] R. Siegel, N. Abramzon, K. Becker, *Electron-impact dissociation and ionization of molecules studied by laser-induced fluorescence techniques*, XXIII ICPIG, Toulouse, France, July 1997, p. I-62-63.

[23] G. Dilecce, S. de Benedictis, *Experimental studies on elementary kinetics in N_2-O_2 pulsed discharges*, Plasma Sources Sci. Technol. **8**(1999)266-278.

[24] G.J. Roth, M.A. Gundersen, *Laser-induced fluorescence images of NO distribution after needle plane pulsed negative corona discharge*, IEEE Trans. Plasma Sci. **27**(1999)28-29.

[25] V. Schultz-von der Gatten, M. Thomson, Ch. Lukas, M. Spaan, H.F. Döbele, *Time and space resolved TALIF-spectroscopy of N-atoms in a dielectric barrier discharge with steep voltage rise*, HAKONE VII, Greifswald, Germany, September 2000, p. 194-198.

[26] A. Pott, T. Doerk, J. Uhlenbusch, J. Ehlbeck, J. Höschele, J. Steinwandel, *Polarization-sensitive coherent anti-Stokes Raman scattering applied to the detection of NO in a microwave discharge for reduction of NO*, J. Phys. D: Appl. Phys. **31**(1998) 2485-2498.